Akatsuki Orbit Determination in Cruising and Venus Approaching Phase

Shiro Ishibashi, Chiaki Aoshima, Yosuke Yamamoto, Tomoko Yagami
Fujitsu Limited
3-9-1 Nakase, Mihama-ku, Chiba-shi, Chiba 261-8588, Japan
and
Makoto Yoshikawa, Hiroshi Takeuchi, Tsutomu Ichikawa, Takaji Kato, Nobuaki Ishii
The Institute of Space and Astronautical Science, JAXA
3-1-1 Yoshinodai, Sagamihara, Kanagawa, 229-8510, Japan

Abstract

The Venus explorer "Akatsuki" has been launched by JAXA in May 21, 2010. After the closest approach to Venus in December 7, Akatsuki is now cruising in interplanetary space. In this paper we describe the following three topics concerning to the orbit determination of Akatsuki. (1) Orbit determination and its precision in Venus approaching phase, (2) The effect of DDOR data on orbit determination precision, (3) Evaluation of Doppler data noise in conjunction phase.

惑星間航行および金星接近フェーズにおける「あかつき」軌道決定

摘要

2010 年 5 月 21 日に打上げられた金星探査機「あかつき」は、12 月 7 日に金星最接近点を通過した後、惑星間航行を続けている。本稿では「あかつき」の軌道決定運用に関して、以下の３つのトピックスについて論ずる。(1)金星接近フェーズの軌道決定と精度評価、(2)DDOR 併用軌道決定におけるデータ量と決定精度の関係、(3)合運用前後におけるドップラデータノイズの評価。

1. Introduction

The Venus explorer "Akatsuki" has been launched by H-IIA rocket in May 21, 2010, and it passed through the closest approaching point to Venus in December 7. Before and after this flyby, Akatsuki was cruising in interplanetary space. Figure 1 shows the trajectory of Akatsuki from the launch to recent position. The trajectories of the Earth and the Venus are also plotted in ecliptic plane.

In this paper, we present the topics concerning orbit determination of Akatsuki in interplanetary space. In section 2 we describe the orbit determination results in Venus approaching phase, and evaluate orbit determination precision by comparing the determination results carried out by JPL (Jet Propulsion Laboratory). In the next section, the results of orbit determination using DDOR (Delta Differential One-way Range) data are presented. The determination precision with and without DDOR data are compared qualitatively. In section 4 we evaluate Doppler data noise in conjunction phase around June 2011. We finally summarize the conclusions of these topics in section 5.

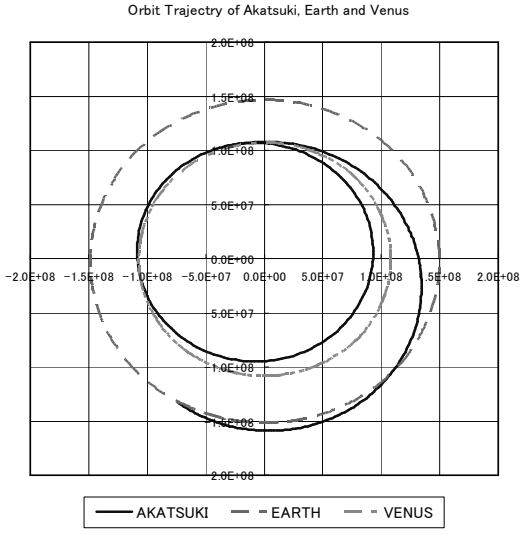

Fig.1 Trajectory of Akatsuki, Earth and Venus

2. Orbit determination in Venus approaching phase

In this section, we present the results of orbit determination in Venus approaching phase. Table 1 shows the orbit determination conditions in this phase. We use X-band range, Doppler, and DDOR data, and estimate state vector and some dynamical parameters simultaneously. For the sake of evaluating orbit determination precision, we also assume the acceleration error corresponding to 5% of radiation pressure.

Figure 2 shows the sequence of trim maneuver and orbit determination in Venus approaching phase. The distance from Akatsuki to the Venus is also depicted in the same figure. The trim maneuvers have been carried out three times, and orbit determinations have been performed twice after each maneuver.

Table 1 Orbit determination conditions for Venus approaching phase

item	condition
tracking data	tracking station : UDSC, USC, DSN tracking data : X-band Range, Doppler, DDOR – Range noise 10 m – Doppler noise 0.3 mm/s – DDOR noise 1×10–9 sec
estimation parameters	– state vector – radiation pressure coefficient (plane model) – unloading (impulse) ΔV – range bias for UDSC and USC
consider parameters	acceleration error – 5×10–12 km/s/s small force in each direction (corresponding to 5% of total radiation pressure)

Fig.2 Sequence of trim maneuver and orbit determination

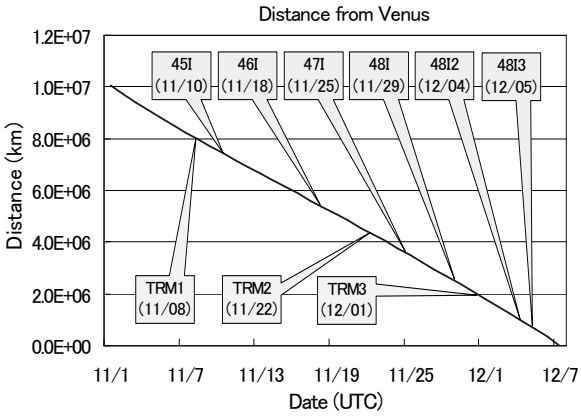

The results of orbit determination are shown in figures 3 to 5. In each figure, the left graph shows the orbit determination result and its error ellipsoid in target b-plane coordinate B_T-B_R. The right graph shows the height from the Venus surface around closest approaching time. For the reference, the orbit determination result obtained by JPL is also plotted in each figure. In almost every case, the orbit determination result by JPL is within the error ellipsoid of ISAS orbit determination result, and it denotes the consistency between these results. The height and the closest approaching time obtained by ISAS and JPL also show similar results for each maneuver case.

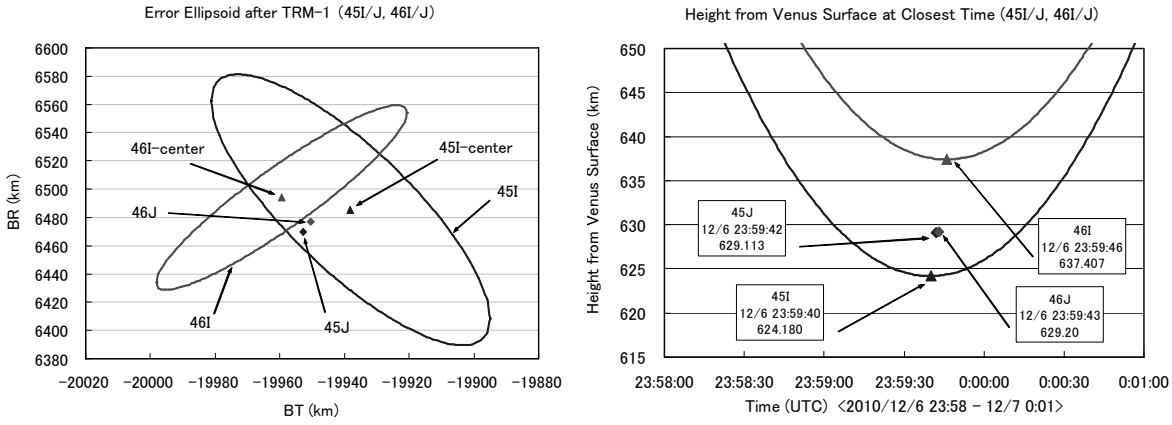

Fig.3 Error ellipsoid after TRM-1 and height from Venus surface at closest time

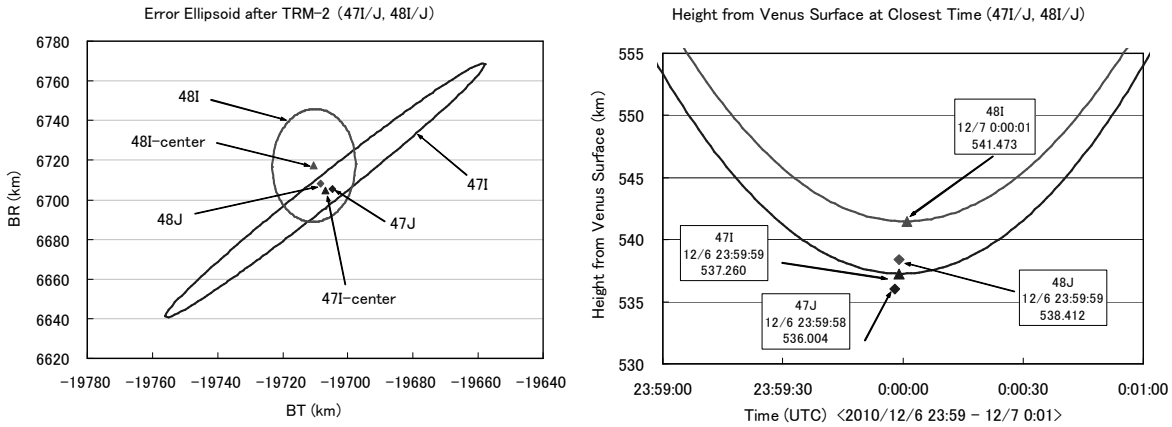

Fig.4 Error ellipsoid after TRM-2 and height from Venus surface at closest time

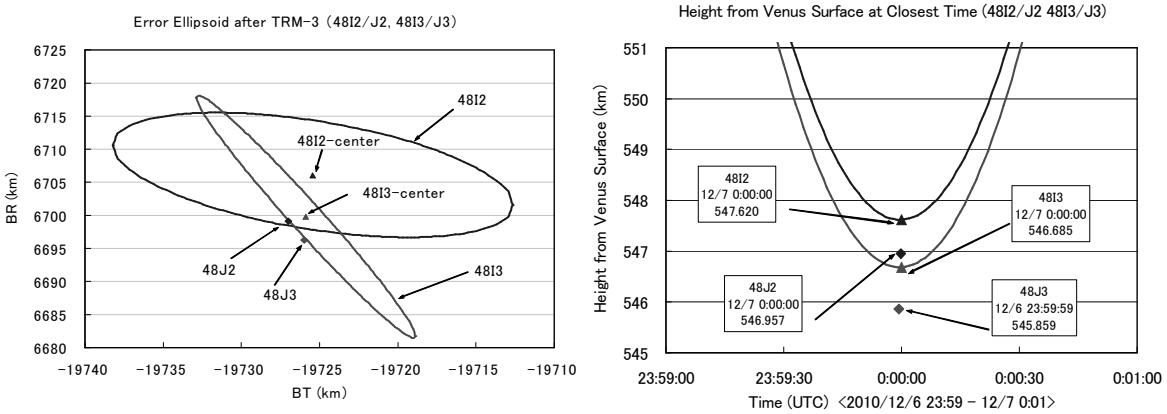

Fig.5 Error ellipsoid after TRM-3 and height from Venus surface at closest time

The precision of orbit determination after three trim maneuvers are summarized in figure 6. The precision of b-plane distance is over 10 km after the first trim maneuver, but it converges to a few km after the third maneuver. The height at the closest approaching point is converged from a few km to within 1 km. The closest approaching time also changes from a few seconds to within 1 sec. This obtained precision is sufficient for Venus insertion operation.

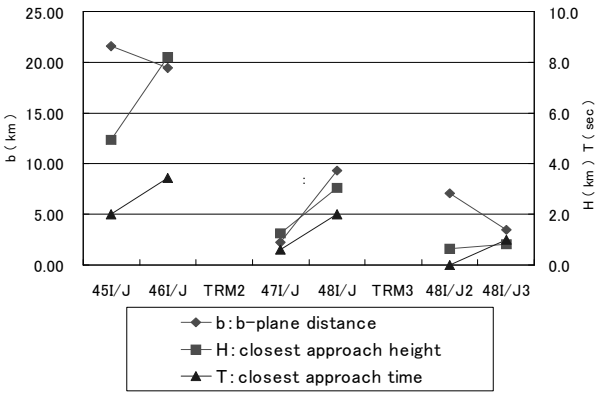

Fig.6 Evaluation of orbit determination precision after TRM-1,2,3

3. Orbit determination with DDOR data

For the next topics, we present the orbit determination results using DDOR data. In cruising phase to the Venus, both ISAS and JPL have performed tracking operation, and exchange obtained tracking data each other. ISAS have carried out orbit determination using both ISAS data and JPL data including DDOR data.

Table 2 DDOR orbit determination conditions

item	condition
tracking data	tracking station : UDSC, USC, DSN tracking data : X-band Range, Doppler, DDOR – Range noise 10 m – Doppler noise 0.5 mm/s – DDOR noise 1×10-9 sec
estimation parameters	– state vector – radiation pressure coefficient (plane model) – unloading (impulse) ΔV – range bias for UDSC and USC
consider parameters	acceleration error – 1×10-12 km/s/s small force in each direction (corresponding to 2% of total radiation pressure)

Table 2 shows the orbit determination conditions in cruising phase. The used observation data are X-band range, Doppler, and DDOR data. We estimate the state vector, range bias, and some dynamical parameters at the same time. For the sake of evaluating determination precision, we consider acceleration error corresponding to 2% of radiation pressure.

The orbit determination cases are summarized in table 3. In this table, orbit determination epoch, data span, and number of range and Doppler data passes obtained by ISAS and DSN (Deep Space Network) are listed respectively. In the next column, we show the position difference between determination results with and without DDOR data. The orbit determination precision with only RARR (Range and Range Rate) data, and that with RARR and DDOR data are also tabulated. The numbers of DDOR data used in orbit determination are shown in the most right column.

Table 3 Number of data passes for DDOR orbit determination

epoch	data span		No. of ISAS pass		No. of DSN pass		position difference (km)	RARR position error (km)	DDOR position error (km)	No. of DDOR data
	start	end	RA2	DP2	SRA	DP2				
2010/7/6 14:00	6/30	7/6	5	6	5	5	0.73	2.56	0.81	6
2010/7/14 14:00	7/8	7/14	4	6	7	7	8.13	3.09	0.87	6
2010/7/21 12:00	7/15	7/21	3	4	7	7	12.43	5.11	0.97	12
2010/7/28 13:00	7/22	7/28	4	5	6	6	0.75	4.48	1.02	12
2010/8/4 10:00	7/29	8/4	2	4	4	4	6.09	7.17	1.47	20
2010/8/11 10:00	8/5	8/11	3	5	3	4	7.61	6.26	2.30	9
2010/8/25 12:00	8/19	8/25	3	5	1	1	5.02	6.55	6.91	2
2010/9/1 11:00	8/26	9/1	5	5	5	5	5.00	6.78	6.14	2
2010/9/15 10:00	9/9	9/15	5	5	2	2	1.40	11.92	11.76	2
2010/9/22 3:00	9/16	9/22	4	4	2	3	1.65	7.76	6.04	1
2010/9/29 11:00	9/22	9/29	5	6	3	3	0.98	13.72	12.34	2
2010/10/6 10:00	9/30	10/6	6	6	3	3	7.25	9.90	5.85	2
2010/10/11 9:00	9/30	10/11	9	9	5	5	2.01	18.77	19.73	2
2010/10/20 8:00	10/14	10/20	5	5	2	2	3.12	8.82	11.58	2
2010/10/27 8:00	10/24	10/27	3	3	2	2	2.49	4.94	4.72	2
2010/11/4 6:00	10/28	11/4	6	6	6	6	5.66	11.50	4.74	6
2010/11/10 23:00	11/8	11/10	3	5	3	3	3.64	6.39	2.32	6

In order to investigate the effect of DDOR data on orbit determination precision, we select the orbit determination cases which have a variety of numbers of DDOR data used. Figure 7 shows the representative 4 results of orbit determination. In each figure the 3 σ error ellipsoid of orbit determination results with only RARR data is depicted with dashed curve in the T-N plane, which is perpendicular to the line of sight. The origin of the coordinate represents the estimated position with only RARR data. In the same figure the error ellipsoid of determination result with RARR and DDOR data is also shown with solid curve, and the estimated position is plotted with the triangle mark. The square mark represents the estimated position by JPL orbit determination.

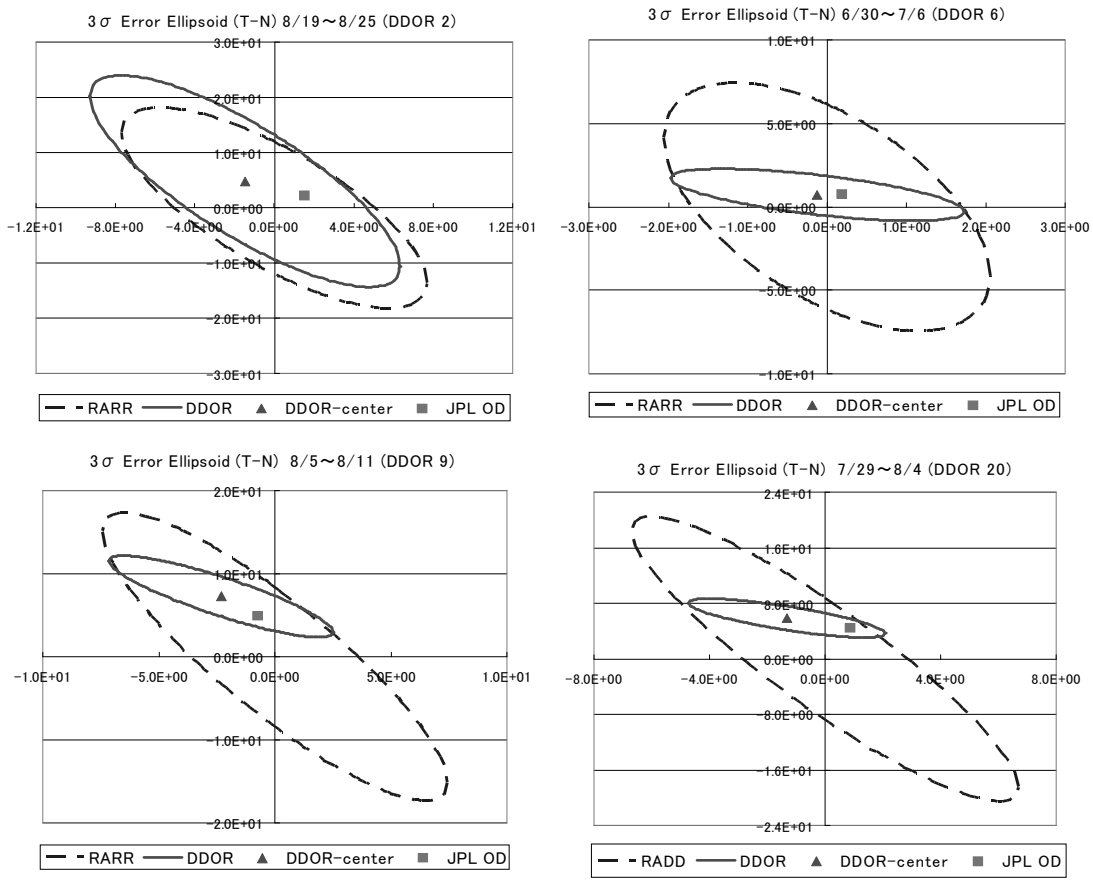

Fig.7 Error ellipsoid of orbit determination results with and without DDOR data

As the numbers of DDOR data used (2, 6, 9, 20 data respectively) are increased, the size of the error ellipsoid becomes smaller. In each case the error ellipsoid with DDOR data is almost within the error ellipsoid with RARR data only, and the estimated positions of both ISAS and JPL orbit determination are also within the error ellipsoid with DDOR data.

Figure 8 shows the relation between the orbit determination precision and the number of DDOR data used. The coordinate of this figure is the ratio of estimation precision with DDOR data to that with RARR data only. As the number of DDOR data used is increased, the estimation precision becomes better, but the precision is almost saturated when the number of DDOR data exceeds over 10.

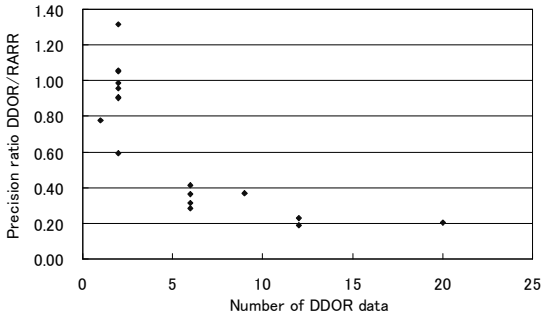

Fig.8 Relation between orbit determination precision and number of DDOR data

4. Doppler data noise in conjunction phase

For the third topics we evaluate the Doppler data noise in conjunction phase. In June 25, 2011 Akatsuki experienced the conjunction, and it was observed behind the sun

around this epoch. In conjunction phase it is well known that the Doppler data noise becomes large when compared with that in the case of normal operation.

Figure 9 shows the change of Doppler residual in orbit determination before and after conjunction epoch. In usual case the typical X-band Doppler noise obtained from UDSC (Usuda Deep Space Center) is within 1 mm/s, but it increases to a several cm/s around conjunction phase. This large Doppler noise is explained by the effect of interplanetary plasma around the Sun.

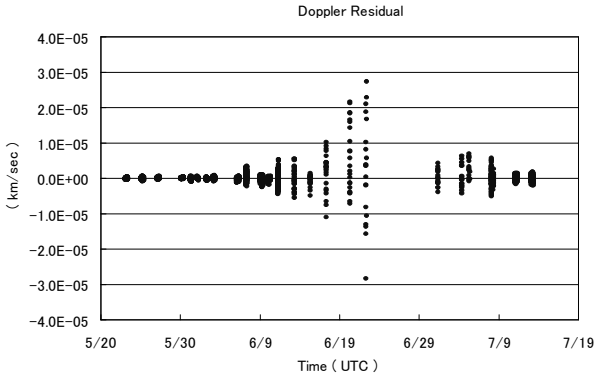

Fig.9 Doppler residual in conjunction phase

In order to evaluate the above observed Doppler noise, we adopt the empirical model developed by NASA/DSN (Deep Space Network) using actual observations. In this model, two-way X-band Doppler noise (Hz) is presented by the following expression.

$$\left(\left\{A_0\left[\frac{\beta}{(\sin\alpha)^{1.3}}\right]F(\alpha,\beta)+A_1\left[\frac{1}{(\sin\alpha)^5}\right]\right\}10^{-A_2\left(|\phi_S|/90\right)}\right)\times 0.26\left\{\frac{60}{\tau}\right\}^{0.3}$$

$$F(\alpha,\beta)=1-0.05\left\{\frac{\left(\beta-\pi/2+\alpha\right)^3-\left(\alpha-\pi/2\right)^3}{\beta}\right\}$$
$$-0.00275\left\{\frac{\left(\beta-\pi/2+\alpha\right)^5-\left(\alpha-\pi/2\right)^5}{\beta}\right\}$$

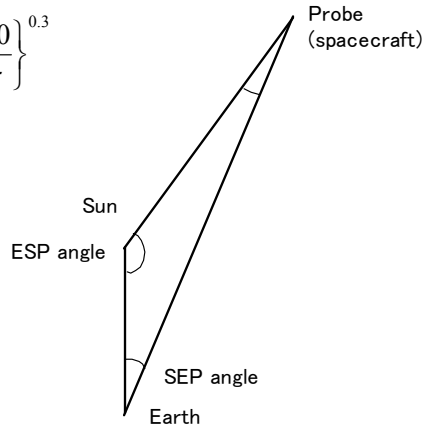

α : SEP angle (rad) β : ESP angle (rad)

ϕ_S : Heliographic latitude (deg) τ : Doppler sampling interval (sec)

$A_0 = 1.18\times10^{-3}$ $A_1 = 4.75\times10^{-10}$ $A_2 = 0.9$

In the above expression the Doppler noise depends on SEP (Sun-Earth-Probe) angle α, ESP (Earth-Sun-Probe) angle β, and heliographic latitude ϕ_S, but SEP angle is the most dominant factor which influences the Doppler noise. By using this expression, we calculate the predicted Doppler noise in the case of the trajectory of Akatsuki, and depict it against SEP angle in figure 10. In the same figure the observed Doppler noise is plotted with a triangle mark. The observed data noise is well represented by the empirical curve.

For comparison the observed noise in the cases of Hayabusa and Nozomi are also plotted with a diamond and a cross mark, respectively in the same figure. For Nozomi data the calibration of frequency dependency are carried out, because the carrier frequency of Nozomi is S-band uplink and X-band downlink. In both spacecraft cases the observed noise is also well fitted by the empirical curve.

When we see figure 10 more precisely, we notice that there are some discrepancy between observed data noise and the empirical curve, especially around SEP ～ 25 deg region, and this tendency is almost common among three spacecrafts. This indicates that the real distribution of the interplanetary plasma is somewhat different from that predicted by empirical model presented above.

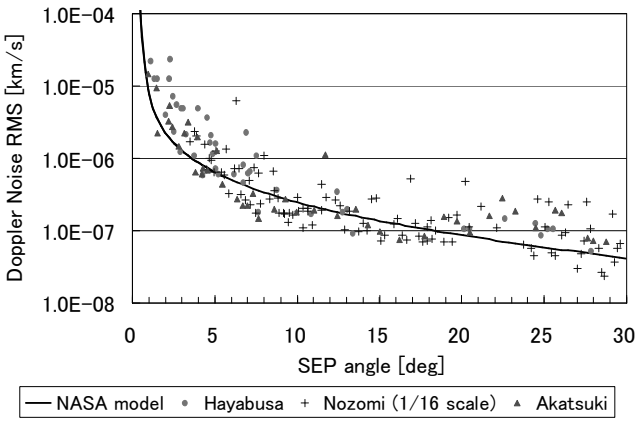

Fig.10 Relation between Doppler data noise and SEP angle

5. Summary and conclusion

In this paper, we present the topics concerning orbit determination of Akatsuki in interplanetary space. The obtained results are summarized as follows.

(1) In Venus approaching phase, we evaluate the orbit determination results after three trim maneuvers. The precision of estimated closest approach height above Venus surface is converged from a several kilometers to within 1 km. The closest approach time is also converged from a few seconds to within 1 sec. The results of orbit determination are also consistent with those performed by JPL. This obtained precision is sufficient for Venus insertion operation.

(2) The orbit determination has been carried out using DDOR data in cooperative operation by ISAS and JPL. By comparing with the results of RARR only cases, it becomes clear that DDOR data is very effective to precise orbit determination, especially in perpendicular to the line-of sight direction. It is also clarified that about 10 data of DDOR observation is sufficient to improve the orbit determination precision.

(3) Doppler data noise in conjunction phase is evaluated precisely. The observed data noise is almost consistent with the empirical model developed by NASA/DSN, but there is some discrepancy between them. This indicates the possibility of improving the distribution model of interplanetary plasma in the future.

References

(1) Nozomi Orbit Determination, T.Ohnishi, S.Ishibashi, M.Yoshikawa, T.Kato, T.Ichikawa, H.Yamakawa, and J.Kawaguchi, 23rd International Symposium on Space Technology and Science, (2002)

(2) HAYABUSA Orbit Determination under Ion Engine Propulsion, T.Ohnishi, S.Ishibashi, M.Yoshikawa, T.Kato, T.Ichikawa, H.Yamakawa, and J.Kawaguchi, 24th International Symposium on Space Technology and Science, (2004)

(3) PLANET-C Orbit Determination in Launch Phase, C.Aoshima, N.Ishii, M.Yoshikawa, H.Takeuchi, T.Ichikawa, T.Kato, T.Yagami, and S.Ishibashi, 20th Workshop on JAXA Astrodynamics and Flight Mechanics, p 205-210 (2010) ISAS

(4) DSN Telecommunications Interfaces：Solar Coronae and Solar Wind Effects, DSN Document 810-5 (1996)